Materials preparation

Chemicals

Hydrochloric acid (HCl), lithium fluoride (LiF), Nitric acid (HNO_3), Ti_3AlC_2, ethanol(C_2H_6O) and Deionized water are purchased from Lanyi Chemical Company (Beijing).

Synthesis of $Ti_3C_2T_x$ nanosheets

Typically, distilled water was added to HCl solution to prepare 9 M HCl. Then, 2 g LiF was added into 9 M HCl solution. After being agitated, 1 g of Ti_3AlC_2 powers with mesh size about 45 μm was slowly added in an ice bath. Immediately followed by magnetic stirring for 24 h at 35 ℃. The resultant was then washed and centrifuged through distilled water addition, until the supernatant reached a pH value of about 6. The precipitate after centrifugation was sonicated in an Ar atmosphere. After the mixture was centrifuged for 1 h at 3500 rpm to eliminate the sediment, the final collected suspension is the few layer $Ti_3C_2T_x$ in the dark supernatant.

Material characterization

The TecnaiTF20 Transmission electron miscroscopy (TEM, Netherlands) was used to investigate the morphologies and microstructure. Energy-dispersive spectroscopy (EDS) element analysis was also performed on the same instrument in TEM mode. The morphology of the active layer was investigated by AFM. The surface areas of MXene were measured by N_2 adsorption at 77 K using a BET surface area analyzer. Contact angle to

detect hydrophilicity. X-ray diffraction (XRD) spectra were collected on D/max-2550 diffractometer with Cu kα- 1radiation (λ = 0.15406 nm). The data of X-ray photoelectron spectroscopy (XPS) were recorded on Kratos Analytical Ltd by using Al Kα, hv = 1486.7 eV.

Electrochemical measurements

The electrochemical properties of supercapacitor and H_2O_2 sensing were carried out in an electrochemical analyzer (CHI 660 D workstation). Ag/AgCl and Pt wire were used as reference and counter electrode, respectively. Cyclic voltammetry (CV), galvanostatic charge-discharge (GCD) and electrochemical impedance spectroscopy (EIS) were conducted in 6 M KOH electrolyte to find the redox activities of the active material towards supercapacitor.

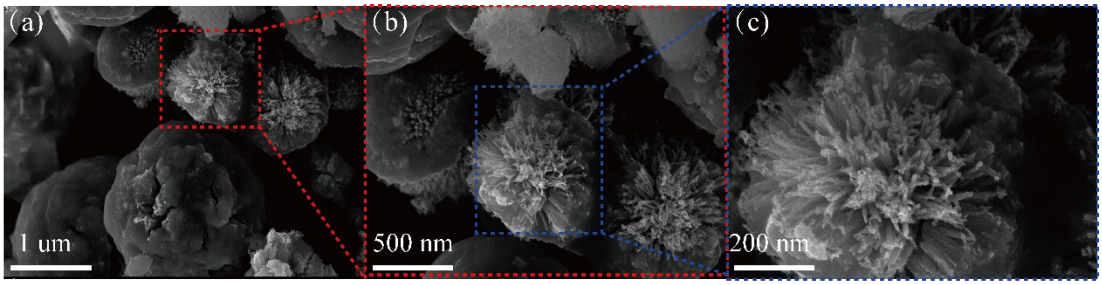

Fig.S1. (a-c) FESEM images of MXene/$NiCo_2S_4$ 1:2 hybrid with different magnification

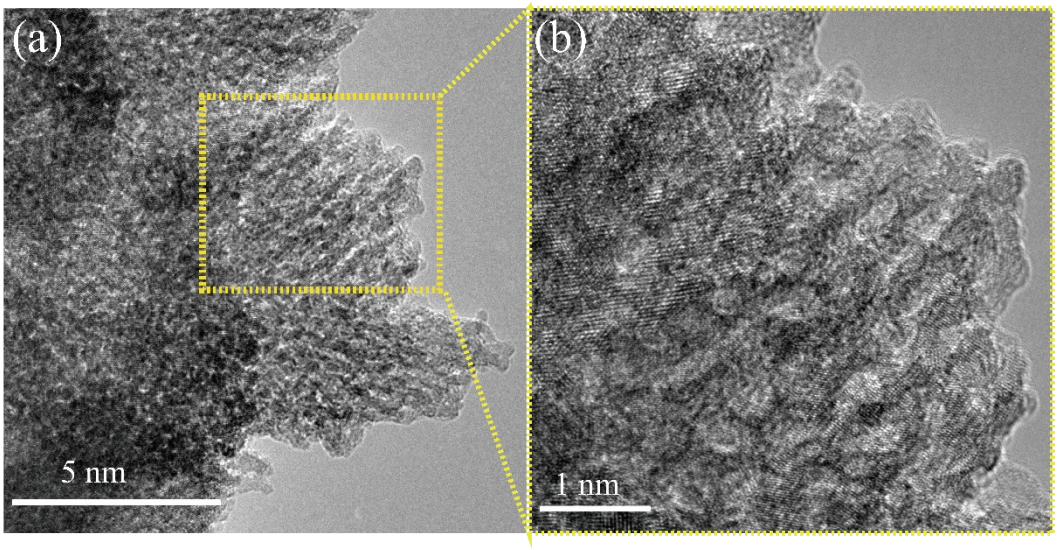

Fig. S2. (a-b)TEM images of MXene/$NiCo_2S_4$ 1:2 hybrid

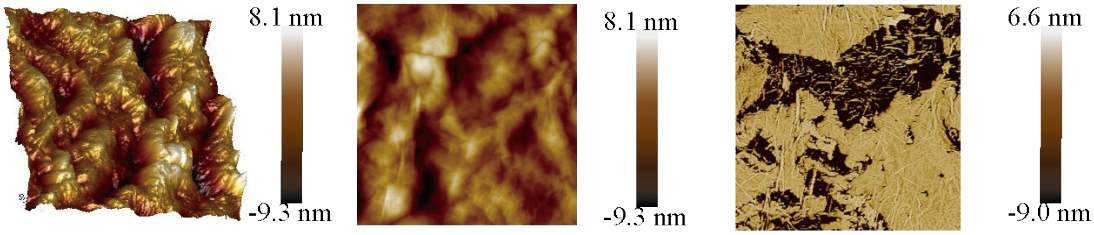

Fig. S3. AFM of pure MXene

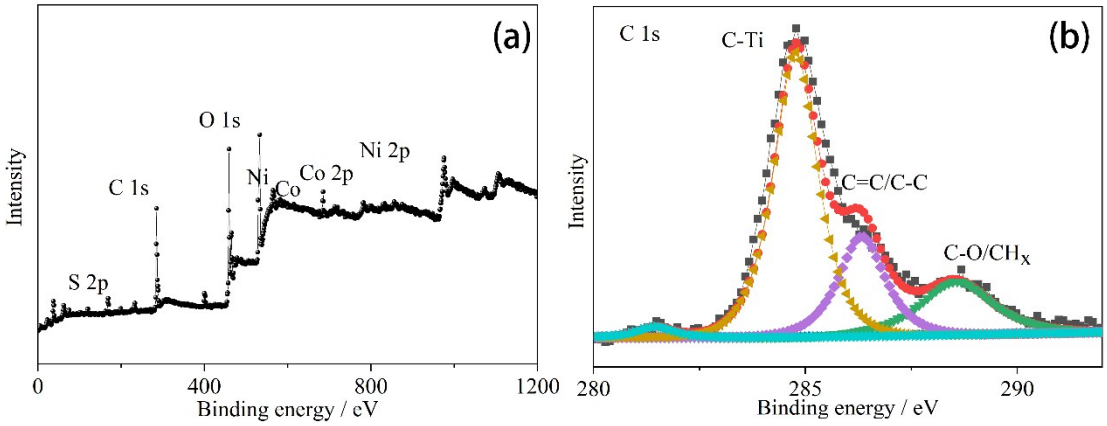

Fig. S4. XPS images of MXene/$NiCo_2S_4$ 1:2 hybrid (a) survey spectrum of MXene/$NiCo_2S_4$ 1:2 hybrid (b) C 1s spectra of MXene/$NiCo_2S_4$ 1:2

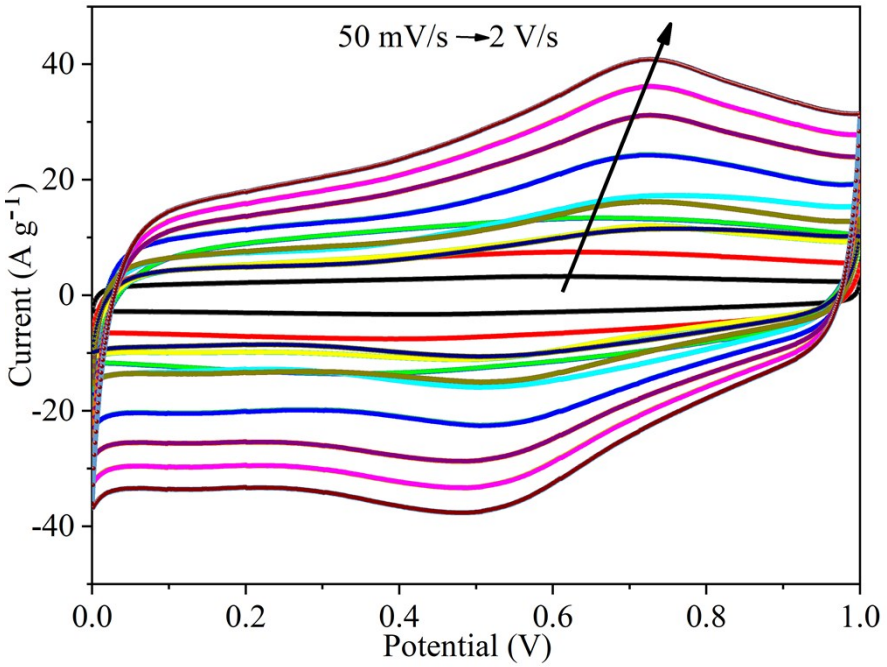

Fig. S5. The CV curves of MXene/$NiCo_2S_4$ 1:2 hybrid at different scan rates.

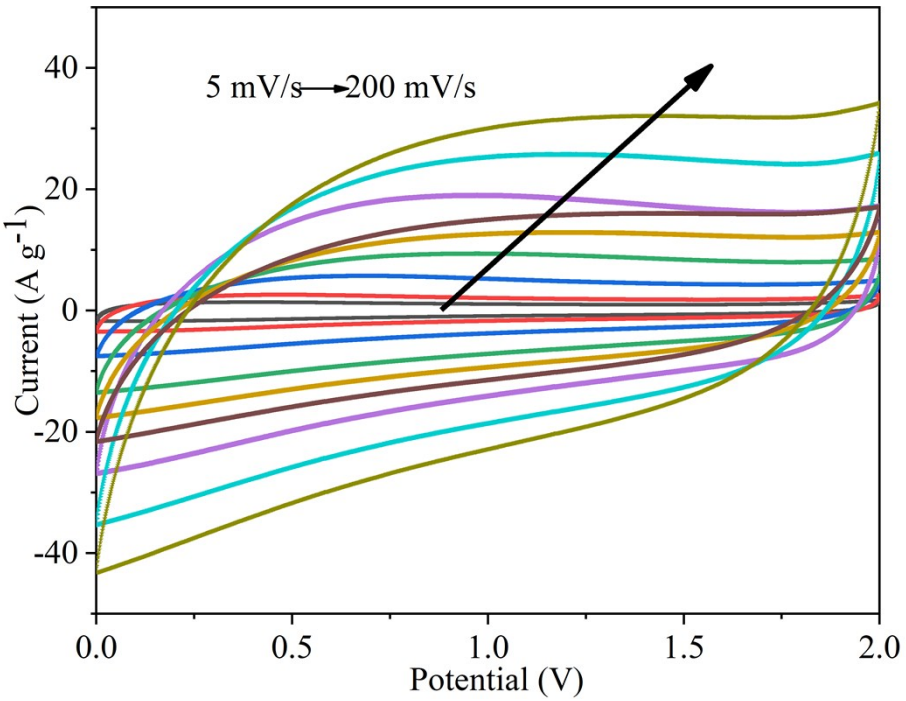

Fig. S6. The CV curves of MXene/$NiCo_2S_4$ 1:2//AAC asymmetric capacitors at different scan rates.

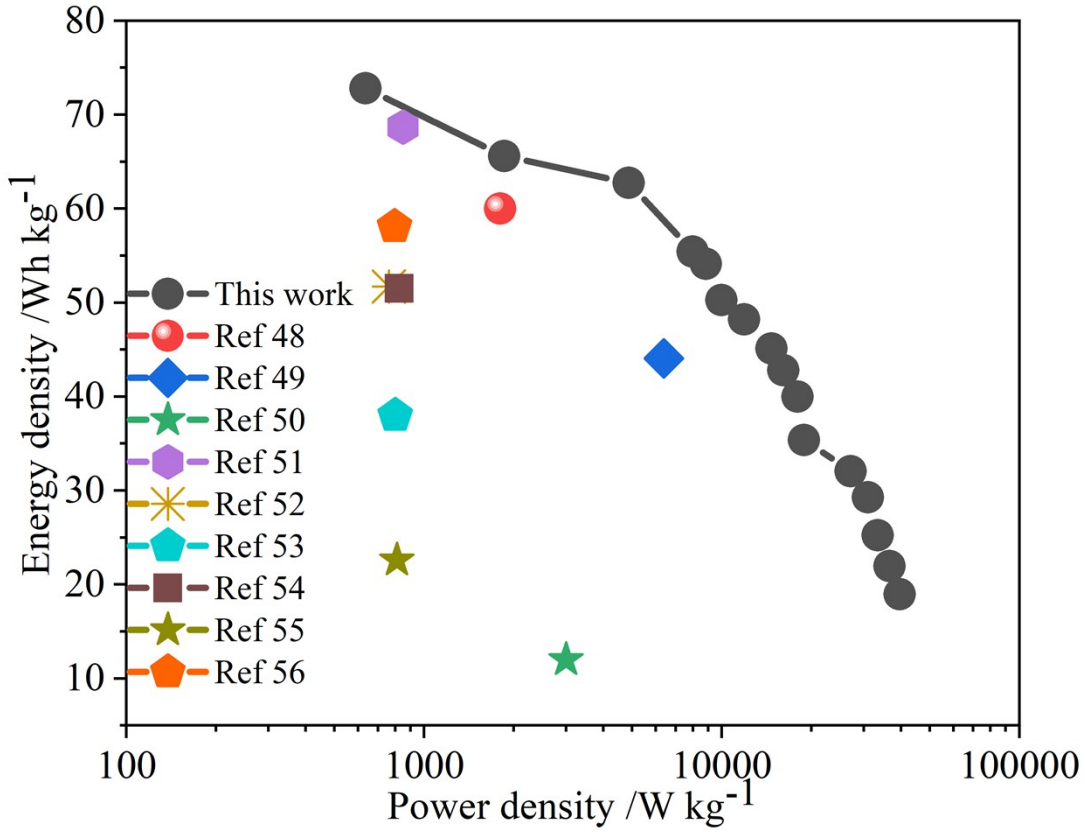

Fig.S7. The comparision of Ragone plot of our work and other Ref.

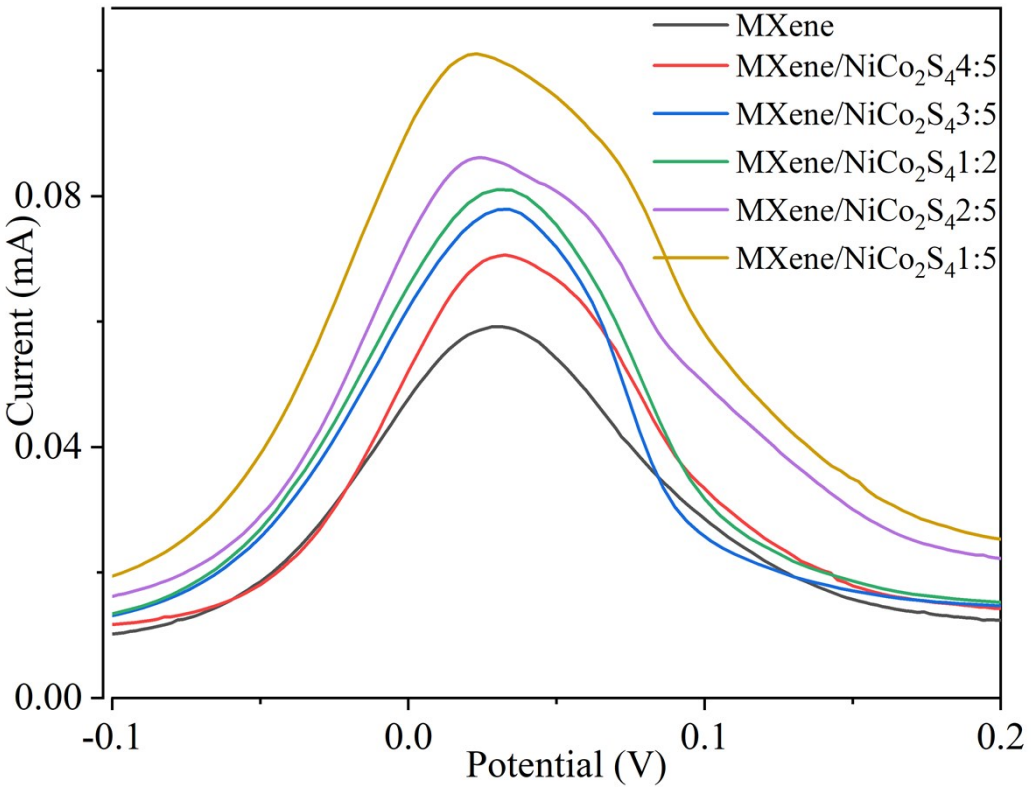

Fig.S8. DPV curves Of MXene and MXene/$NiCo_2S_4$ hybrids for the concentration of H_2O_2(5μM)

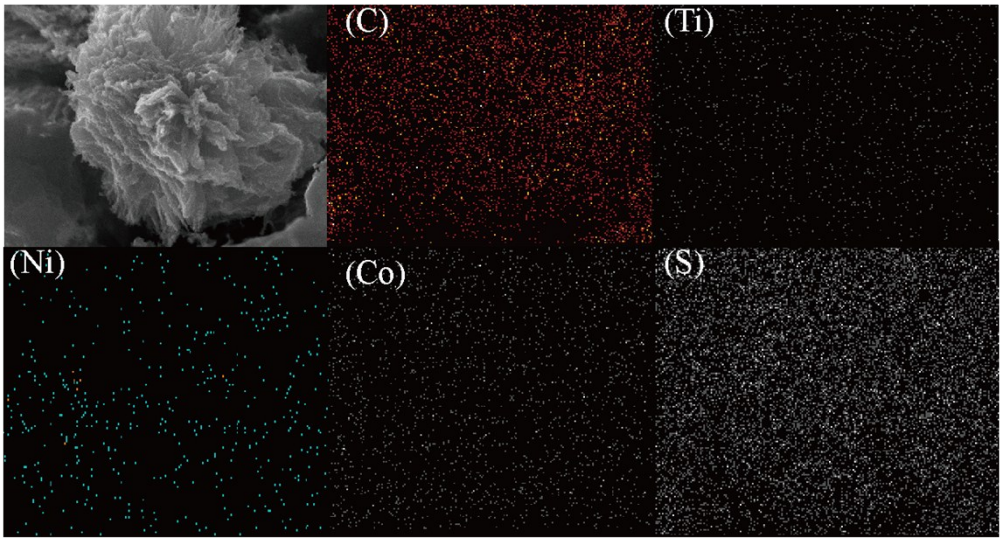

Fig.S9. The elemental mapping measurement of MXene/$NiCo_2S_4$

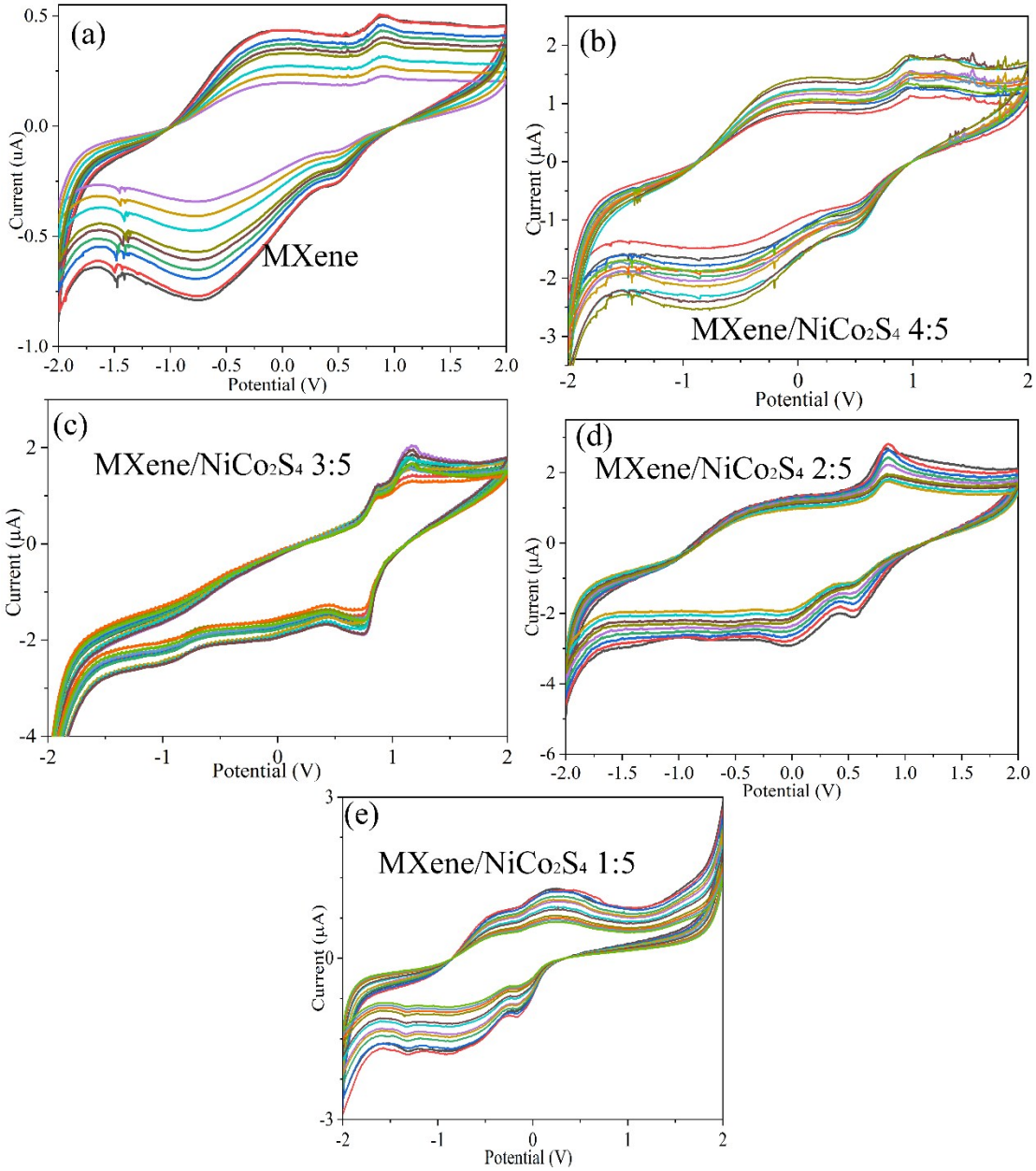

Fig. S10. (a) cyclic voltammograms with different scanning rates of MXene sensor (b) cyclic voltammograms with different scanning rates of MXene/$NiCo_2S_4$ 4:5 sensor (c) cyclic voltammograms with different scanning rates of MXene/$NiCo_2S_4$ 3:5 sensor (d) cyclic voltammograms with different scanning rates of MXene/$NiCo_2S_4$ 2:5 sensor (e) cyclic voltammograms with different scanning rates of MXene/$NiCo_2S_4$ 1:5 sensor